Journal of Orthopaedic Translation 38 (2023) 256–267

Contents lists available at ScienceDirect

Journal of Orthopaedic Translation

journal homepage: www.journals.elsevier.com/journal-of-orthopaedic-translation

Original article

Single-cell RNA sequencing reveals resident progenitor and vascularization-associated cell subpopulations in rat annulus fibrosus

Heng Sun [a], Huan Wang [a], Weidong Zhang [a], Haijiao Mao [c,**], Bin Li [a,b,*]

[a] Department of Orthopaedic Surgery, Orthopedic Institute, The First Affiliated Hospital, Suzhou Medical College, Soochow University, Suzhou, Jiangsu, China
[b] Collaborative Innovation Center of Hematology, Soochow University, Suzhou, Jiangsu, China
[c] The Affiliated Hospital of Medical School, Ningbo University, Ningbo, Zhejiang, China

ARTICLE INFO

Keywords:
Annulus fibrosus
Gene regulation network
Single-cell RNA sequencing
Subpopulation
Stem cell
Vascularization

ABSTRACT

Background: One of the main causes of low back pain is intervertebral disc degeneration (IDD). Annulus fibrosus (AF) is important for the integrity and functions of the intervertebral disc (IVD). However, the resident functional cell components such as progenitors and vascularization-associated cells in AF are yet to be fully identified.
Purpose: Identification of functional AF cell subpopulations including resident progenitors and vascularization-associated cells.
Methods: In this study, the single-cell RNA sequencing data of rat IVDs from a public database were analyzed using Seurat for cell clustering, gene ontology (GO) and Kyoto Encyclopedia of Genes and Genomes (KEGG) for functional analysis, StemID for stem cell identification, Monocle and RNA velocity for pseudotime differentiation trajectory validation, single-cell regulatory network inference and clustering (SCENIC) for gene regulatory network (GRN) analysis, and CellChat for cell–cell interaction analysis. Immunostaining on normal and degenerated rat IVDs, as well as human AF, was used for validations.
Results: From the data analysis, seven AF cell clusters were identified, including two newly discovered functional clusters, the *Grem1*$^{+}$ subpopulation and the *Lum*$^{+}$ subpopulation. The *Grem1*$^{+}$ subpopulation had progenitor characteristics, while the *Lum*$^{+}$ subpopulation was associated with vascularization during IDD. The GRN analysis showed that *Sox9* and *Id1* were among the key regulators in the *Grem1*$^{+}$ subpopulation, and *Nr2f2* and *Creb5* could be responsible for the vascularization function in the *Lum*$^{+}$ subpopulation. Cell–cell interaction analysis revealed highly regulated cellular communications between these cells, and multiple signaling networks including PDGF and MIF signaling pathways were involved in the interactions.
Conclusions: Our results revealed two new functional AF cell subpopulations, with stemness and vascularization induction potential, respectively.
The Translational potential of this article: These findings complement our knowledge about IVDs, especially the AF, and in return provide potential cell source and regulation targets for IDD treatment and tissue repair. The existence of the cell subpopulations was also validated in human AF, which strengthen the clinical relevance of the findings.

1. Introduction

Low back pain (LBP) is the leading cause of years lived with disability worldwide [1]. One of the main causes of LBP is intervertebral disc degeneration (IDD) [2,3]. However, the treatment for IDD is still limited due to an insufficient understanding of the intervertebral disc (IVD). IVD is an avascular tissue composed of gel-like nucleus pulposus (NP) in the center, annulus fibrosus (AF) around NP, and cartilaginous endplates (CEPs) at the top and bottom of IVD. Among them, AF has a complicated structure according to the multilayer fibers, different extracellular matrix (ECM) components, and variant cell morphology [4], implicating the heterogeneity of AF cell functions. However, although cell heterogeneity was reported in AF [5], the functional cell components are yet to be fully identified in this tissue, hindering the understanding of AF, as well as strategy formulation for tissue repair.

Tissue regeneration includes a series of processes such as

* Corresponding author. 178 Ganjiang Rd, Rm 201 Bldg 18, Soochow University (North Campus), Suzhou, Jiangsu, 215007, China.
** Corresponding author.
E-mail addresses: maohaijiao@nbu.edu.cn (H. Mao), binli@suda.edu.cn (B. Li).

https://doi.org/10.1016/j.jot.2022.11.004
Received 8 August 2022; Received in revised form 8 November 2022; Accepted 15 November 2022

inflammation, cell migration and differentiation, ECM remodeling, angiogenesis, etc. [6] To have a better understanding of AF tissue and accelerate the tissue repair process, it is necessary to figure out the relevant resident cells. Several reports have demonstrated the existence of AF-specific stem/progenitor cells, as stem and/or progenitor cells are significant in tissue homeostasis maintenance and damage repair, but no clear consensus has been made [4,7,8]. Recently, mouse, rat, human, and bovine IVD cells were analyzed with single-cell RNA sequencing (scRNA-seq), and the stem/progenitor cells were identified in these species respectively using the mesenchymal stem cell markers [9–13]. Nevertheless, these studies didn't identify AF resident progenitors, which may help the regeneration of the damaged IVDs. Therefore, it is essential to find out and characterize the AF-specific stem/progenitor cells. Gremlin 1, a secreted antagonist of bone morphogenetic proteins, was reported to mark stem cells in the musculoskeletal system [14]. These stem cells self-renew and generate osteoblasts, chondrocytes, and reticular marrow stromal cells. As IVD has a close relationship with cartilage and bone, it could be interesting to explore if *Grem1* labels stem/progenitor cells in IVDs as well.

Nutrition supply is another factor that affects tissue metabolism and homeostasis. As mature AF is avascular except for the outmost layer, it receives the nutrition supply mainly from diffusion, and other regulators such as hormones, cytokines, and immune cells are less effective [15]. However, when IDD occurs, the blood vessels will invade the inner layer of AF, bringing more cells and regulation factors to the tissue [16]. Lama et al. found that vascularization of the AF in IDD was confined in the disrupted ECM area, indicating that the AF components could be responsible for vascularization [17]. Therefore, clarifying the vascularization in AF is another indispensable part of understanding IVDs. However, the function and contribution of the AF cells for vascularization are yet to be elucidated.

ScRNA-seq is a very useful tool to explore the heterogeneity of the cells in tissues, and rat, mouse, human, and bovine IVD scRNA-seq analyses have been done recently [5,9–12], giving us a great opportunity to reveal the cell components in IVDs, especially in the AF. With this tool, Wang et al. introduced their excellent work by providing rat IVD cell atlas and potential new gene markers for NP and AF cell subpopulations, as well as a new potential stem cell subpopulation [10]. Based on the published rat data, we further analyzed the cell components of AF, aiming to identify the progenitor-like and vascularization-associated cell subpopulations, respectively. The key regulators were also analyzed to give us a comprehensive understanding of the newly identified cell subpopulations. This study expands our understanding of the AF and its cell components, which may in return provide new strategies for IDD treatment, as well as tissue regeneration.

2. Methods and materials

2.1. Single-cell sequencing and data analysis

The single-cell data were accessed from the public database Gene Expression Omnibus (GEO) (GSE154884), with the pooled healthy AF and NP cells from 4 male and 4 female rats of 8-week-old [10]. The gene expression matrix file was downloaded and imported into R studio (version 1.4) software. The cells with detected gene numbers between 200 and 4,000, and total counts less than 20,000 were selected for further analysis. Clustering was performed using Seurat 4.0 (https://satijalab.org/seurat/), with the dimension reduction performed by principal component analysis (PCA), and visualized by Uniform Manifold Approximation and Projection (UMAP). In brief, the Seurat object was generated from digital gene expression matrices. Twenty principal components were used in IVD cell clustering with the resolution parameter set at 0.05, while in AF cell clustering the resolution parameter was set at 0.4. Gene ontology (GO) and Kyoto Encyclopedia of Genes and Genomes (KEGG) enrichment analyses were performed on the Metascape website (https://metascape.org/) [18], with genes of average logFC >0.3 for the whole IVD cells, and logFC >0.5 for AF cells. For KEGG result presentation, irrelevant disease terms were excluded to specify the cell functions and signaling pathways. Stemness analysis was performed by StemID, the algorithm that scores the cell clusters with connectivity and transcriptome entropy. StemID infers the lineage tree and identifies stem cells from single-cell sequencing data [19,20]. Pseudotime analysis was performed by Monocle [21,22] from Cole Trapnell Lab, and the genes with average logFC >0.8 were used for ordering cells. The cell differentiation trajectory was validated by RNA velocity using velocyto. R [23]. The gene regulation network (GRN) analysis was performed using the single-cell regulatory network inference and clustering (SCENIC) algorithm, which is a computational method for simultaneous GRN reconstruction and cell-state identification from scRNA-seq data and has been widely used in a variety of single-cell studies [9,24,25]. The expression matrix was filtered for genes available in RcisTarget's database (mm9-tss-centered-10kb). The regulon data was then analyzed using the RcisTarget package to create TF motifs using the mm9-tss-centered-10kb database. The regulon activity scores were calculated using Area Under the Curve (AUC) function. Predicted target genes of regulon were ranked by Genie3Weight value and filtered by normalized enrichment score (NES) of binding motifs. The transcriptional network of TF and predicted target genes were visualized by Cytoscape (v3.8.2). Cell–cell interaction analysis was performed by CellChat [26]. The unmentioned parameters were all default in these analyses.

2.2. Animal model

To show the existence of the cell subpopulations *in vivo*, the rat IVD degeneration model was used. Animal experiments were approved by the Institutional Animal Care and Use Committee of Soochow University. The compression model was established in our previous study as it simulates the overload of the IVDs, and this model has been fully characterized before [27,28]. Briefly, fifteen 3-month-old male Sprague–Dawley rats were randomly divided into control (n = 5) and compression (n = 10) groups. For the compression group, the caudal vertebrae of the rats were immobilized with a custom external device fixing four vertebrae (Co7-10), and the distance of Co8-9 vertebrae was shortened by 1 mm to compress the IVD between the vertebrae for 4 or 8 weeks. For the control group, the vertebrae were fixed without compressing the IVDs. The rats were sacrificed 4 or 8 weeks after the device fixation, and the specimens were collected for further investigations.

2.3. Histological staining

To show the effect of compression on IVDs, safranin O/fast green staining was used. Tissues for histology and immunostaining were fixed in 4% (w/v) paraformaldehyde (Absin, China) for 24 h before decalcification in 10% (w/v) ethylene diamine tetraacetic acid (EDTA) (Solarbio, China) solution. Subsequently, the specimens were embedded in paraffin and sliced (7 μm) for further safranin O/fast green staining or immunostaining. The sections were then deparaffinized and stained by hematoxylin (Sigma–Aldrich, USA) for 20 min, followed by fast green (Sigma–Aldrich, USA) staining for 8 min, acetic acid washing for 1 s, and safranin O (Sigma–Aldrich, USA) staining for 8 min subsequently. Finally, the slides were mounted with neutral resin (Sigma–Aldrich, USA) and scanned before observation.

2.4. Immunostaining

To indicate the cell subpopulation locations in AF, immunohistochemistry (IHC) and immunofluorescence (IF) were used. Human AF tissue was obtained from an IDD patient who underwent discectomy with the patient's consent. For IHC, Paraffin sections were treated with 0.25% trypsin (Gibco, USA) for 30 min in a 37 °C incubator or 0.01 M citrate for 8 h in a 60 °C incubator, followed by 3% (v/v) hydrogen peroxide (South

Land Pharmaceutical, China) for 15 min at room temperature (immunohistochemistry only), blocking buffer (containing bovine serum albumin, detergent, and Triton X-100; Beyotime, China) for 1 h at room temperature, primary antibodies (Gremlin 1: Santa Cruz, USA, sc-515877; ID1: Santa Cruz, USA, sc-133104; Lumican: Absin, China, abs136805; IGF-1: Absin, China, abs148500) overnight, and secondary antibodies (anti-rabbit HRP: Beyotime, China, A0208; anti-mouse HRP: Multi Sciences, China, GAM0072) for 2 h at room temperature, subsequently. The slides were washed with PBS for 5 min three times between steps. The DAB substrate system (ZSGB-bio, China) was used for color development. Hematoxylin staining was utilized to reveal the cell nuclei. Then the slides were mounted with neutral resin and observed with a microscope (Carl Zeiss, Germany). For IF, antigen retrieval was followed by blocking directly before primary antibody incubation (IGF-1: Santa Cruz, USA, sc-518040; ID1: Absin, China, abs133269; PDGFRA, Absin, abs136347). Secondary antibodies (anti-mouse AlexaFluor 488: Absin, China, abs20014; anti-Rabbit Cy3: Absin, China, abs20024) were incubated at room temperature for 2 h. The sections were mounted with Antifade Mounting Medium with DAPI (Beyotime, China, P0131) before observation with a microscope (Carl Zeiss, Germany). For quantitative analysis, 3 sections from each sample were selected, and the positive/total cell ratio was calculated for each section.

2.5. Statistical analysis

The quantitative data are presented as mean ± standard deviation. The Student's *t*-test was utilized for the two-group comparison. The statistical analysis of the single-cell data was performed using the built-in algorithm in the packages. Values of $p < 0.05$ were considered to be statistically significant.

3. Results

3.1. AF cell identification and selection

The IVD single-cell gene expression matrix file was downloaded and imported into R studio (version 1.4) software for analysis. The distributions of total counts and detected genes per cell were first calculated

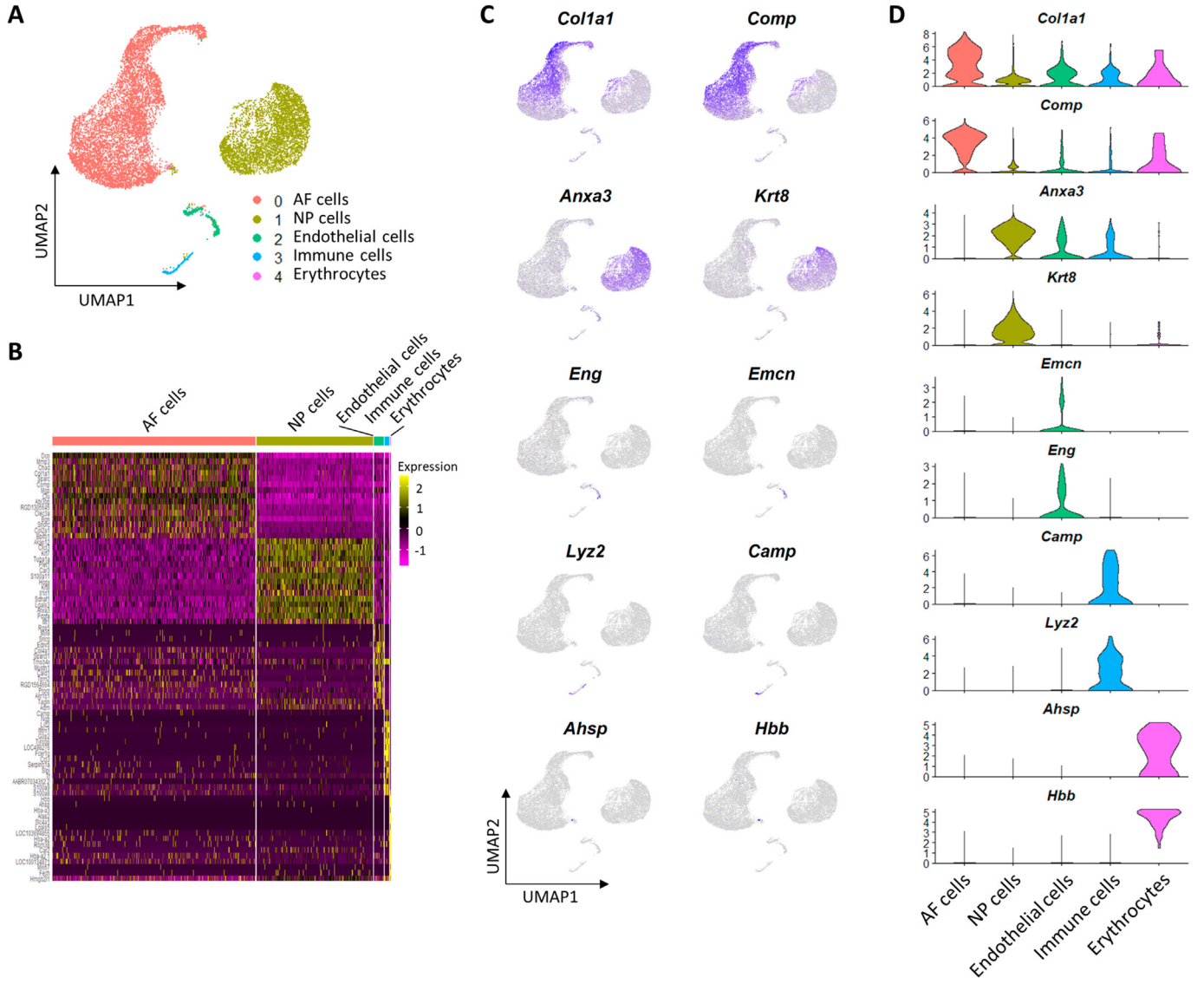

Figure 1. Heterogeneity of the rat IVD cells (A) Featureplot of IVD cell cluster distribution visualized by UMAP. Each dot indicates a cell. AF cells, NP cells, endothelial cells, immune cells, and erythrocytes were identified (B) Heatmap of the differentially expressed genes for each cluster. Each row indicates a gene, and each column indicates a cell (C) Featureplots showing the distribution of the representative genes. Blue color intensity indicates the expression level of the gene in corresponding cells (D) Violin plots showing expression levels of the representative genes for each cluster.

(Fig. S1A). After quality control, 13,566 cells expressing 15,407 genes were selected for further analysis, while 13,578 cells expressing 17,401 genes were detected in the original article [10]. Using Seurat, the IVD cells were clustered into 5 clusters, with two major clusters and three minor clusters. The clustering recapitulated the original article and was visualized by UMAP (Fig. 1A). The differentially expressed genes (DEGs) of these clusters are demonstrated in the heatmap (Fig. 1B) and Table S1. With the highly expressed marker genes in each cluster, we were able to identify these cells (Fig. 1C and D, and S1B). Cluster 0 was identified as AF cells based on the markers *Col1a1*, *Comp*, and *Dcn* [12,29]. Cluster 1 was considered as NP cells according to the high expression of *Krt8, Anxa3*, and *Lgals3* [12,30,31]. Cluster 2 was speculated as endothelial cells because *Eng, Emcn*, and *Cdh5* encode endoglin, endomucin, and vascular endothelial cadherin, the three endothelium markers, respectively [32–34]. *Lyz2, Camp,* and *Ngp* are expressed in immune cells which fit cluster 3 [35–37], and the hemoglobin-related genes *Hbb, Ahsp,* and *Hba-a2* demonstrated the identity of the last cluster, erythrocytes. The gene ontology (GO) analysis based on the highly expressed genes of each cluster confirmed the identity of the functional cell clusters: "blood vessel morphogenesis" for endothelial cells, "inflammatory response" for immune cells, and "gas transport" for erythrocytes (Fig. S1C). The list of GO analysis is demonstrated in Table S2. Interestingly, Wang et al. identified cluster 2 as stem-like cells in the original article, indicating that some cells in this cluster had stemness. The stem cell marker *Eng* was previously identified as a functional marker that defines hematopoietic stem cells [38]. Thus, it is not surprising that these cells had both stem and endothelial cell characteristics.

To explore the heterogeneity of AF cells, cluster 0 was selected for the following analyses.

3.2. Heterogeneity of AF cells

The AF cells were further clustered into seven subclusters by Seurat (Fig. 2A and B), and the marker genes are demonstrated in Fig. 2C and D, and S2, while listed in Table S3. In the original article, Wang et al. got four clusters since they mainly focused on the differences between inner and outer AF cells, therefore less attention was paid to functional subpopulation exploration [10]. Among these seven subclusters, the well-known AF cell subpopulations were found based on the top DEGs, such as inner layer AF cells (iAFCs) (*Col2a1, Sod2*) [11] and outer layer AF cells (oAFCs) (*Col1a2, Col1a1*). The iAFCs also expressed *Agt*, the gene that encodes angiotensinogen, the precursor of angiotensin, indicating that these cells may play a regulatory role in AF through the tissue renin-angiotensin system [39], and the GO and KEGG analysis showed an active response of the iAFCs to environmental stimuli indicated by "chemotaxis" and "chemokine signaling pathway" -related terms (Fig. S2A). oAFCs expressed abundant ECM genes including *Fmod*, *Sparc*, *Col11a1*, and so on, in line with the GO and KEGG analysis results that the ECM organization and interaction came to the top of the lists (Fig. S2B). The inflammation-associated cells (IACs) (*Plat, Nos2*) and the redox-associated cells (RACs) (*Nqo1, Txnrd1*) were also presented since *Plat* and *Nos2* are inflammatory-related factors (Fig. S2C) [40,41], and *Nqo1*, as well as *Txnrd1*, participate in the redox process (Fig. S2D) [42,43]. The GO and KEGG analysis showed that "inflammatory response"

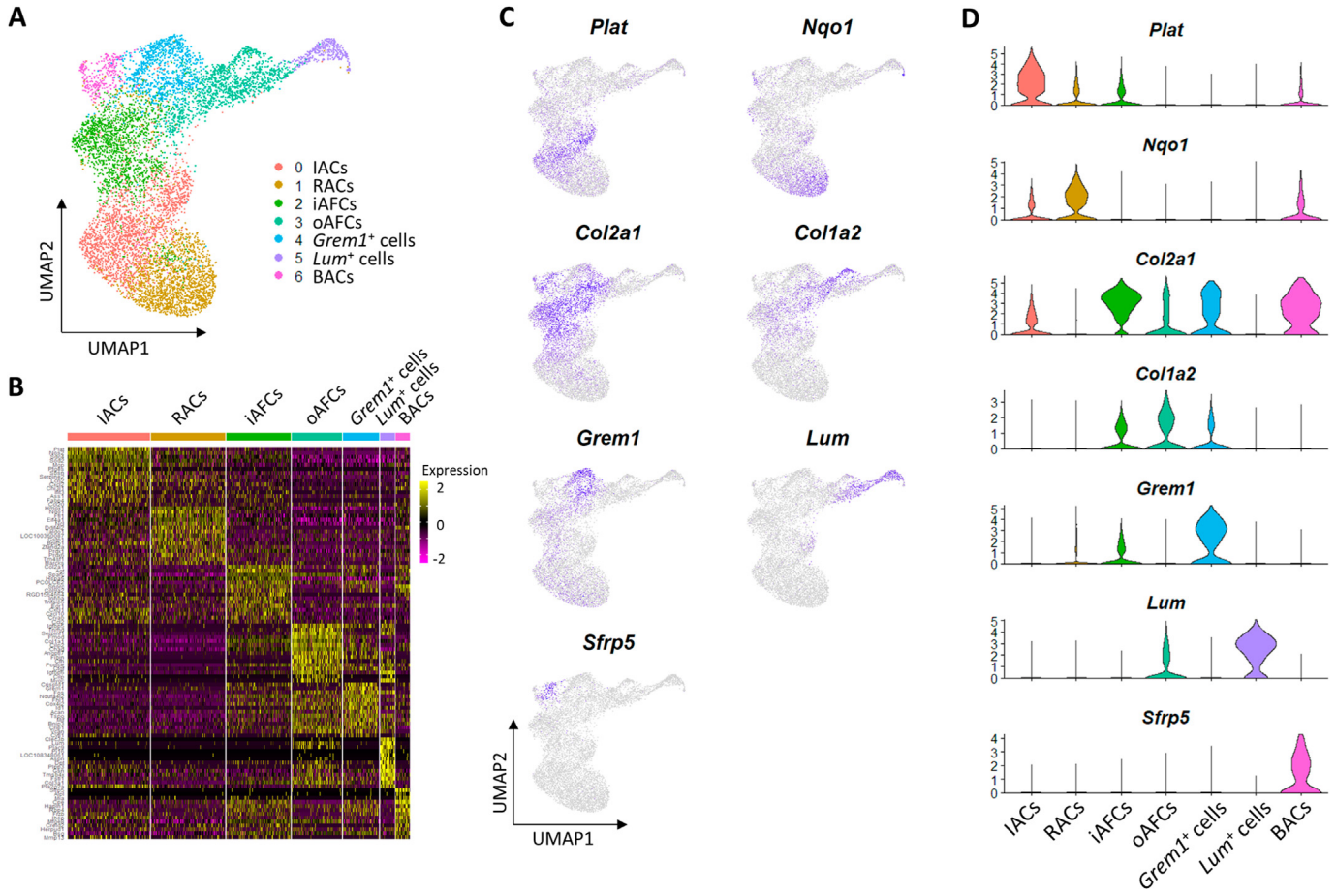

Figure 2. Heterogeneity of rat AF cells (A) Featureplot of AF cell clusters visualized by UMAP. IACs, RACs, iAFCs, oAFCs, *Grem1*$^{+}$ cells, *Lum*$^{+}$ cells, and BACs were identified (B) Heatmap of the differentially expressed genes for each cluster. Each row indicates a gene, and each column indicates a cell (C) Featureplots showing the distribution of the representative genes. Blue color intensity indicates the expression level of the gene in corresponding cells (D) Violin plots showing expression levels of the representative genes for each cluster.

and "TNF signaling pathway" were associated with IACs, while "cell redox homeostasis" and "ferroptosis" were related to RACs, demonstrating the inflammation and redox-associated characteristics of these subpopulations. The presence of IACs and RACs in the normal AF tissue indicates that inflammation and redox could be related to maintaining tissue homeostasis. In fact, redox homeostasis and inflammation both exist in physiological conditions [44,45]. Since the IVDs locate next to vertebrae, it was not surprising to see bone-associated cells (BACs) (*Sfrp5*, *Alpl*), which expressed *Alpl* encoding alkaline phosphatase and *Ibsp* encoding bone sialoprotein II (Fig. S2E). All the significant GO and KEGG terms are also listed in Table S4. Interestingly, there were two newly discovered subpopulations: *Grem1*$^{+}$ cells, and *Lum*$^{+}$ cells. Since *Grem1* is a marker of stem cells, and the *Lum*$^{+}$ cell cluster expressed several vascularization-associated genes, which show functional characteristics respectively, we next looked into these two subpopulations.

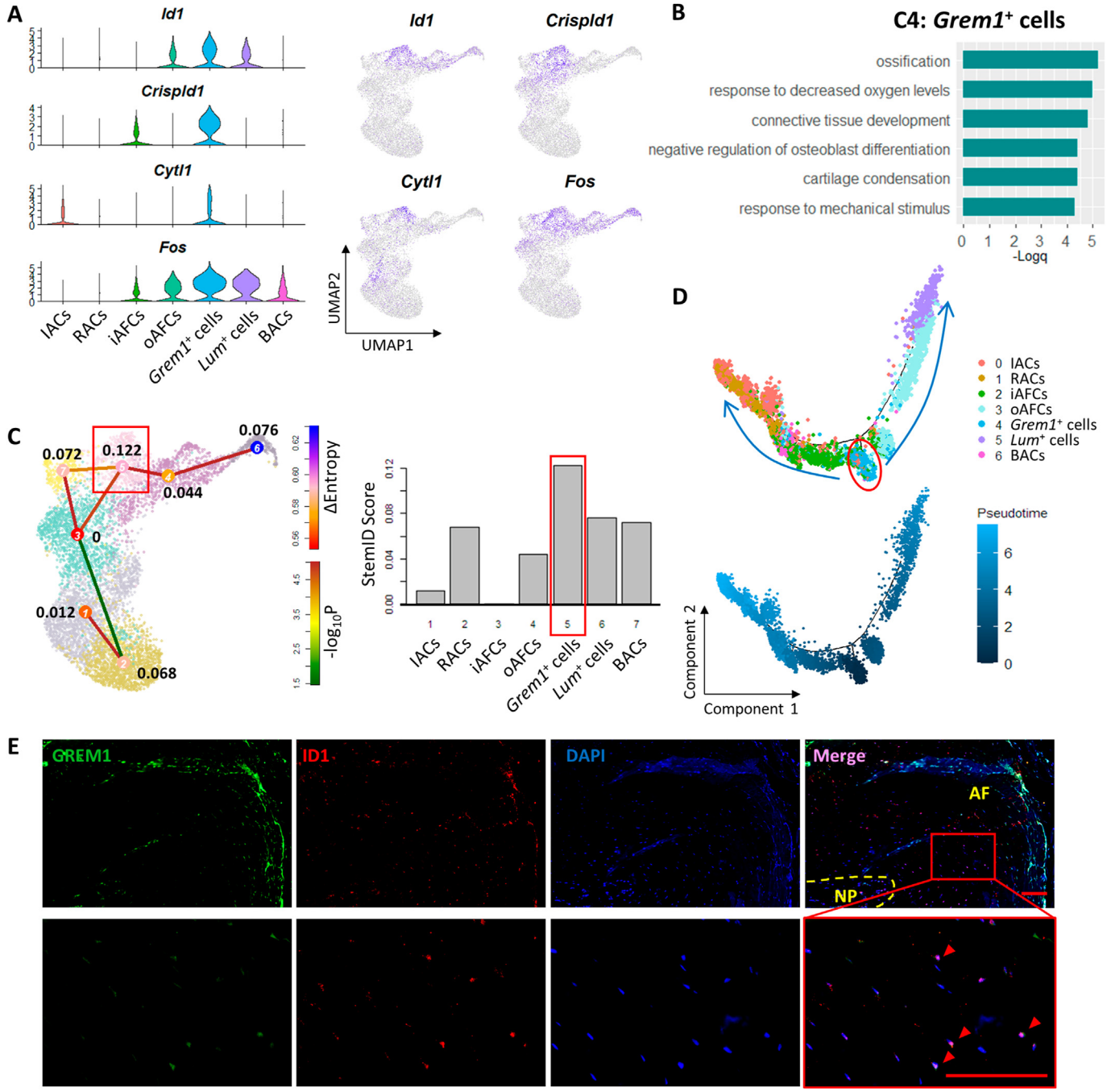

Figure 3. Progenitor characteristics of the *Grem1*$^{+}$ cell subpopulation (A) Violin plots and featureplots showing expression levels and distribution of the representative genes of the *Grem1*$^{+}$ cluster. Blue color intensity indicates the expression level of the gene in corresponding cells (B) Enriched GO terms of the differentially expressed genes in *Grem1*$^{+}$ cluster. The terms were ranked by -logq values (C) Inferred AF lineage tree visualized in the UMAP-embedded space. The color of the link indicates the -logP value. The color of the vertices indicates the entropy. The red rectangular frame indicates the *Grem1*$^{+}$ cell cluster. The StemID scores are presented in the histogram, as well as the featureplot (D) Pseudotime trajectory inferred by Monocle and colored according to cell subpopulations (upper plot) or pseudotime (lower plot). The red circle indicates *Grem1*$^{+}$ subpopulation; the arrows indicate differentiation directions (E) Immunofluorescent staining of GREM1 and ID1 showing the presence of the cells in rat AF tissue. Arrows indicate the double-positive cells. Scale bar, 100 μm. AF, annulus fibrosus; NP, nucleus pulposus.

3.3. The progenitor characteristics of Grem1$^+$ cells in AF

Grem1 was recently reported to mark skeletal stem cells [14]. Meanwhile, the *Grem1*$^+$ cell cluster expressed AF ECM genes like *Col2a1*, *Col1a2* as well as *Fmod*. Therefore, we speculated that the *Grem1*$^+$ subpopulation was the resident progenitor cells in AF. Apart from *Grem1*, this subpopulation co-expressed *Id1*, *Cripsld1*, *Cytl1*, and *Fos* (Fig. 3A). *Id1* was reported to be expressed in less differentiated chondrocytes, and it plays a key role in the regulation of cell-cycle progression and cell differentiation in chondrocytes and other cells [46–48]. *Crispld1* is important for hematopoietic stem cell self-renewal [49]. *Cytl1* is important for chondrogenesis and cartilage development [50]. *Fos* was implicated as a regulator of cell proliferation and differentiation in the skeletal system [51]. These co-expressed genes sketched the *Grem1*$^+$ subpopulation with stemness characteristics. Additionally, GO analysis showed that these cells were related to cell differentiation and tissue development (Fig. 3B), and KEGG analysis showed that genes of "TGF-β signaling pathway" and "signaling pathways regulating pluripotency of stem cells" were enriched in this subpopulation (Fig. S3A).

To further validate our hypothesis, the StemID algorithm was applied [19]. StemID infers the lineage tree and identifies stem cells from scRNA-seq data, with high entropy indicating the permissive stem cell transcriptome and direct links of one cluster to others reflecting transcriptome plasticity. The final StemID score indicates the potential of being stem cells. Using this method, we found that the *Grem1*$^+$ cell subpopulation had the highest potential to be the stem cells since this cluster got the highest StemID score of 0.122 (Fig. 3C). This subpopulation had the highest direct link number, with the second-highest Δentropy (Fig. 3C, S3Bappsec1, and S3C). In line with this, the pseudotime analysis using Monocle got a similar result that *Grem1* cell cluster (red circle) went to either oAFCs and *Lum*$^+$ cells (right blue arrow), or iAFCs, IACs, and RACs (left blue arrow) (Fig. 3D and S3D). RNA velocity result was consistent with Monocle that the arrows started from *Grem1* cell cluster to iAFCs or oAFCs (Fig. S3E). Interestingly, the IACs and RACs may be further differentiated from iAFCs based on the Monocle pseudotime trajectory and the RNA velocity plot, implying a possible pattern of homeostasis maintenance by the differentiated cells, which remains to be validated. Immunostaining demonstrated the existence of this subpopulation in the healthy rat AF by double-staining of GREM1 and ID1, with a positive rate of 14.0 ± 5.7% (Fig. 3E). These data support our hypothesis that the *Grem1*$^+$ cells could be the resident progenitor subpopulation in AF.

3.4. The vascularization-associated characteristics of Lum$^+$ cells

Lum$^+$ cells specifically expressed several markers including *Igf1*, *Angptl1*, *Ackr3*, *Pdgfra*, *Col4a1*, *Fbn1*, *Ecm1*, *Col3a1*, *Mmp14*, *Cd34*, etc. (Fig. 4A and S4A) These markers are all associated with vascularization. IGF-1 was reported to promote angiogenesis in endothelial cells [52]. *Angptl1* encodes angiopoietin-like 1, a member of the vascular endothelial growth factor family [53]. Atypical chemokine receptor CXCR7 (ACKR3) promotes developmental and pathological angiogenesis [54]. PDGFRα also mediates angiogenesis and connective tissue remodeling [55]. Type Ⅳ collagen and fibrillin, the products of *Col4a1* and *Fbn1* respectively, are also the vascular ECM proteins [56]. Additionally, GO analysis indicated that this subpopulation was related to epithelial cell proliferation and vasculature development (Fig. 4B); KEGG analysis indicated that this cluster had a high metabolic level (Fig. S4B). Therefore, the *Lum*$^+$ cells are supposed to be associated with vascularization.

It is well-known that the IVD is generally an avascular tissue in physiological conditions, with only a few blood vessels in the outmost layer of AF and adjacent endplates. When degeneration occurs, the AF would be vascularized from the outmost layer to the inner layers [16]. Hence, we investigated if the *Lum*$^+$ cell subpopulation was associated with vascularization during degeneration using the rat tail compression model, since this model imitates mechanical overloading on the IVDs, one of the major causes of IDD in humans [57]. This animal model has been built and validated as described previously [28]. The Safranin O/fast green staining showed that the rat IVDs remarkably degenerated after 8 weeks of compression: the NP was cracked, and the AF layers were disorganized with the loss of proteoglycan, demonstrating a successful IDD model (Fig. 4C). To locate the *Lum*$^+$ cell subpopulation, the immunohistochemistry of lumican (LUM) was performed, and the result showed that some LUM positive cells were presented near the boundary of AF and endplate, but they can hardly be seen in the out layer, especially the central out layer of AF (Fig. 4D, red square). When the IVD has degenerated, more LUM-positive cells were presented in the outer and inner layers of the AF (Fig. 4D), consistent with the invasion process of the blood vessels. In line with this, the IGF-1 level was also up-regulated in the outer layer in the degenerated IVD group (Fig. S4C). Additionally, LUM$^+$ cells located close to VEGFA$^+$ cells in degenerated AF, further indicating the relevance of *Lum*$^+$ cell subpopulation and vascularization (Fig. 4E). To validate the temporal invasion process of the *Lum*$^+$ cells during degeneration, the LUM$^+$ IGF-1$^+$ cells were marked by immunofluorescence in the IVDs of 4 weeks and 8 weeks post-surgery. The result showed that the double-positive cells were increased in a time-dependent manner (Fig. 4F). In comparison, the *Grem1*$^+$ progenitors didn't show significant quantitative or locational changes during degeneration (Fig. S4D). These data imply that the *Lum*$^+$ cell subpopulation could be associated with vascularization in the AF, especially in the degeneration condition.

We also explored the existence of the LUM$^+$ and GREM1$^+$ cells in human AF. Consistent with rats, LUM$^+$ cells, as well as GREM1$^+$ ID1$^+$ cells, were presented in the degenerated human AF, and LUM$^+$ cells were located in the outmost layer, suggesting a similar function of these subpopulations in humans, although IGF-1 was not co-localized with LUM (Fig. 4G). These data indicate a translational potential of our findings.

3.5. Gene regulation network and cell–cell interactions of the two cell subpopulations

To further understand the characteristics of the two new subpopulations of interest, we used SCENIC to investigate the GRN [24]. The activated regulons in each subpopulation were found and presented in the heatmap (Fig. 5A), as well as listed in Table S5. The cell-type-specific regulons were calculated and named by the key transcription factors (TFs) (Fig. 5B). The top 5 regulons in *Grem1*$^+$ progenitor cells were *Tcf7l1*, *Hoxc10*, *Id1*, *Hes6*, and *Sox9* (Fig. 5B and C, and S5A). *Tcf7l1* regulates cell differentiation in embryonic stem cells [58], and *Sox9* is not only the key TF in chondrocytes but also a stemness regulator in intestine and cancer [59,60]. The corresponding target genes of the regulons (Table S6) were then picked out for GO and GRN analyses. The GO analysis result demonstrated that these target genes were related to tissue development and cell differentiation (Fig. 5D and Table S7), and the GRN showed that the key target genes including *Sox6*, *Grem1*, *Cytl1*, *Fgfr2*, *Acan*, etc. Were regulated by the top regulons (Fig. 5E). These data further suggest that the *Grem1*$^+$ cells is a stem cell-like cell subpopulation.

The top 5 regulons in *Lum*$^+$ vascularization-associated cells (VACs) were *Nfic*, *Creb5*, *Nr2f2*, *Rarb*, and *Bhlhe41* (Fig. 5B and F, and S5Bappsec1). *Nr2f2* is responsible for vascular morphogenesis during development [61]. *Creb5* promotes angiogenesis in colorectal cancer [62]. In line with the previous results, GO analysis of the target gene also showed that they were enriched in vasculature development (Fig. 5G and Table S8). The GRN demonstrated a more complex regulation of the top regulons to the highly related genes including *Igf1*, *Angptl1*, *Angpt1*, *Angpt2*, *Pdgfra*, *Vwf*, *Cd34*, *Col4a1*, *Fbn1*, etc (Fig. 5H). These data indicate the angiogenic function of the *Lum*$^+$ cell subpopulation.

The signaling network among the AF cell subpopulations and other main IVD cell clusters was investigated by cell–cell interaction analysis using CellChat. The results demonstrated highly regulated cellular communications between these cells (Fig. 5I). The significant outgoing

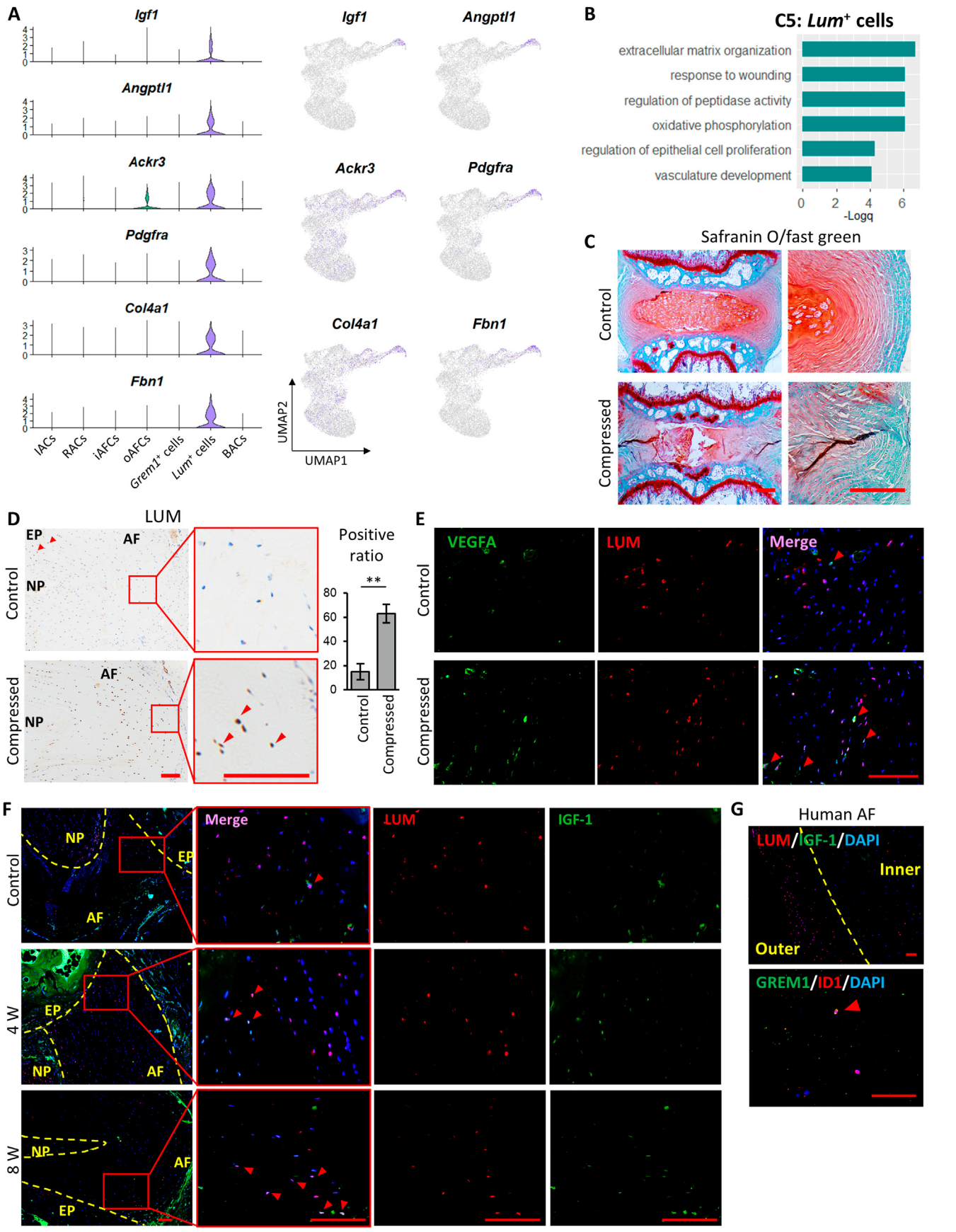

(caption on next page)

Figure 4. Vascularization-associated characteristics of the *Lum*$^+$ cells (A) Violin plots and featureplots showing expression levels and distribution of the representative genes of the *Lum*$^+$ cluster (B) Enriched GO terms of the differentially expressed genes in *Lum*$^+$ cluster. The terms were ranked by -logq values (C) Safranin O/fast green staining of the rat intervertebral discs 8 weeks post-surgery. Scale bar, 100 μm (D) Immunohistochemistry staining showing the presence of the LUM$^+$ cells in normal and compressed rat AF tissues. Arrows indicate the representative positive cells. Scale bar, 100 μm $^{**}p < 0.01$. AF, annulus fibrosus; NP, nucleus pulposus; EP, endplate (E) Immunofluorescent staining showing the co-localization of LUM$^+$ and VEGFA$^+$ cells in normal and compressed rat AF tissues. Arrows indicate the VEGFA$^+$LUM$^-$ cells. Scale bar, 100 μm (F) Immunofluorescent staining showing the LUM$^+$IGF-1$^+$ cells in normal, 4 weeks post-surgery, and 8 weeks post-surgery rat AF tissues. The arrows indicate the double-positive cells. Scale bar, 100 μm (G) Immunofluorescent staining showing the location of LUM$^+$ cells and GREM1$^+$ cells in degenerated human AF. Arrow indicates the GREM1$^+$ID1$^+$ cells. Scale bar, 100 μm.

and incoming signaling patterns were listed in Fig. S5C. Among these communication signals, PDGF signaling, which was previously mentioned in VAC characterization and GRN analysis, was found in the interactions between VACs and other cells (Fig. 5J). Interestingly, NP cells were inferred to be the most significant signal sender of PDGF signaling. Considering the spatial distance of NP cells and VACs, it would be worth investigating if the NP cells can regulate vascularization through the AF barrier. Another significant signaling regulating VACs was MIF, in which the progenitor and oAFC subpopulations were the significant signal senders (Fig. 5K). The MIF signaling pathway is reported strongly implicated in inflammation and angiogenesis [63], in line with the VAC function. Compared with other AF cells, the progenitors were less regulated by other IVD cell clusters and AF subclusters (Fig. S5C), while it was supposed to regulate IACs, RACs, iAFCs, and even NP cells by SPP1 signaling (Fig. S5D). SPP1 is well-known for its function in bone formation [64], and it also contributes to cell behavior in a variety of cell types [65,66], which gives us a hint that the progenitors may maintain tissue homeostasis not only by its stemness but also through conducting cell behavior within the tissue. These data sketch the complex regulating network within the AF.

4. Discussion

IDD affects millions of people around the world but the clinical intervention strategy is limited. One important reason could be an insufficient understanding of the IVD tissue, especially the AF. In our study, we decoded mature rat AF cell components and identified two novel cell subpopulations: *Grem1*$^+$ progenitor cells and VACs, providing new knowledge and potential therapeutic targets for clinical practice. With more understanding of the IVDs, tissue regeneration by utilizing the resident progenitor cells, or disease progressing regulation by manipulating vascularization, may become feasible strategies for IDD treatment in the future.

The single-cell RNA sequencing data of rat IVDs was previously analyzed by Wang et al. who discovered several new biomarkers for both NP and AF cells, as well as a stem cell population [10]. Based on their published data, we dug into the AF cells and further identified two functional AF subpopulations that could be responsible for tissue repair and regeneration—the *Grem1*$^+$ progenitors and the *Lum*$^+$ vascularization-associated cells, and revealed the key regulators of the two subpopulations. In line with our discovery, Wang et al. also identified the inner and outer AF cell subpopulations by *Col1a1* and *Col2a1*, and the inflammatory and immune-responsive cell subclusters were found, similar to our IAC and RAC subpopulations. Our data further identified two functional AF cell subpopulations, which complemented the results of the AF in the original article. Panebianco et al. analyzed the AF cell populations in bovine IVDs as well, and part of their results was shared with ours, such as the oAF and iAF markers (*Col1a1*, *Col1a2*, and *Igfbp6*; *Col2a1*, *Sod2*, and *Mgp*) (Fig. S6) [11]. Similarly, Calió et al. analyzed the bovine IVD scRNA-seq and the bulk RNA-seq data, and a stem cell-like cluster (cluster 10), as well as a vascular cell-like cluster (cluster 8), was found in the AF [12]. Wang et al. identified mouse AF stem cells and progenitor cells between the epiphyseal plate and AF [5]. Following their analysis of the AF cell atlas, our in-depth study further indicates the existence of the two cell subpopulations in AF tissue. However, discrepancy also exists. Gan et al. performed single-cell analysis on human NP, AF, and CEP, and they found that human NP and AF cells were both mainly chondrocyte-like cells, and the differences between AF and NP are much less than in rats and bovines [9]. This discrepancy reflects the diversity of the tissue composition in different species.

Stem and progenitor cells have been found in AF tissue, but there are no committed markers specifically for these cells [4]. In this study, we found the *Grem1*$^+$ cell subpopulation which had the progenitor characteristics, providing additional proof for the existence of stem/progenitor cells in AF tissue. Consistently, *Grem1* was reported to be the marker of a population of osteochondroreticular stem cells as well as intestinal reticular stem cells [14]. Another highly expressed gene of this subpopulation, *Id1*, is important in the development and embryonic stem cell self-renewal maintenance [48,67]. These data indicate that the *Grem1*$^+$ cell subpopulation could be an AF progenitor, and gremlin 1 is a potential marker to identify AF-derived stem/progenitor cells, making the stem/-progenitor cell identification in AF more accurate. Similarly, Gan et al. and Tu et al. found progenitor subpopulations in human NP tissue respectively [9,13]; Wang et al. identified stem cells and progenitor cells near mouse AF [5], all supporting our hypothesis that there are tissue-specific stem/progenitor cells in the IVDs. In the original article, Wang et al. identified another cluster, the *Eng* and *Mcam* positive stem-like cells with multi-differentiation capability [10]. However, from their analysis, this subpopulation was derived from neither AF cells nor NP cells, indicating that they may not be resident stem cells. Because *Eng* was a functional marker that defines hematopoietic stem cells [38], it is not surprising to see these cells with both stem and endothelial cell characteristics. Consistently, Wang et al. decoded the mouse AF cell atlas and found a CD105 (*Eng*)-positive stem cell subpopulation, which expressed neither *Col1a1* nor *Col2a1* [5]. These cells were located adjacent to the epiphyseal plate and regarded as a cell source for AF [5]. Our analyses, together with Wang et al. complement the cell atlas of the rat IVDs. As AF-derived stem cells can be regulated by the topography of biomaterials [68], the combination of biomaterials with intrinsic stem/progenitor cells can be a new strategy for tissue repair.

The mature IVDs are considered to be avascular, but the IVDs in children and young adults are with blood vessels [16,69]. Additionally, the avascular mature IVDs would be vascularized during degeneration [16,70]. Our study reveals that the *Lum*$^+$ cell subpopulation is associated with AF vascularization during IDD, indicating that the AF cells may actively participate in this process. In line with our results, Gan et al. found that endothelial cells and pericytes communicated with NP progenitor cells via VEGF, PDGF, and TGF-β signaling pathways [9], suggesting that the resident IVD cells are capable of regulating vascularization. Calió et al. also showed that a subcluster of AF (cluster 8) had the highest similarity to vascular endothelial cells [12]. Vascularization during IDD occurs from AF and endplates [71], consistent with our result that the *Lum*$^+$ cells were located near the endplates. Feng et al. found that the AF cells have multilineage differentiation potential, indicating that they could have distinct functions, including angiogenesis [72]. Le Maitre et al. found that IGF-1, one of the growth factors that was highly expressed in the *Lum*$^+$ cell subpopulation, was associated with blood vessel ingrowth in degenerated inner AF [73], demonstrating the relationship between IGF and vascularization. IGF and PDGF are two important signals for vascular smooth muscle cell migration and blood vessel formation [74]. Our findings, together with others, further suggest the vascularization-associated cell subpopulation in AF, providing a possible target for vascularization interference in IVDs.

However, it is still not clear if vascularization is good or bad for IVDs.

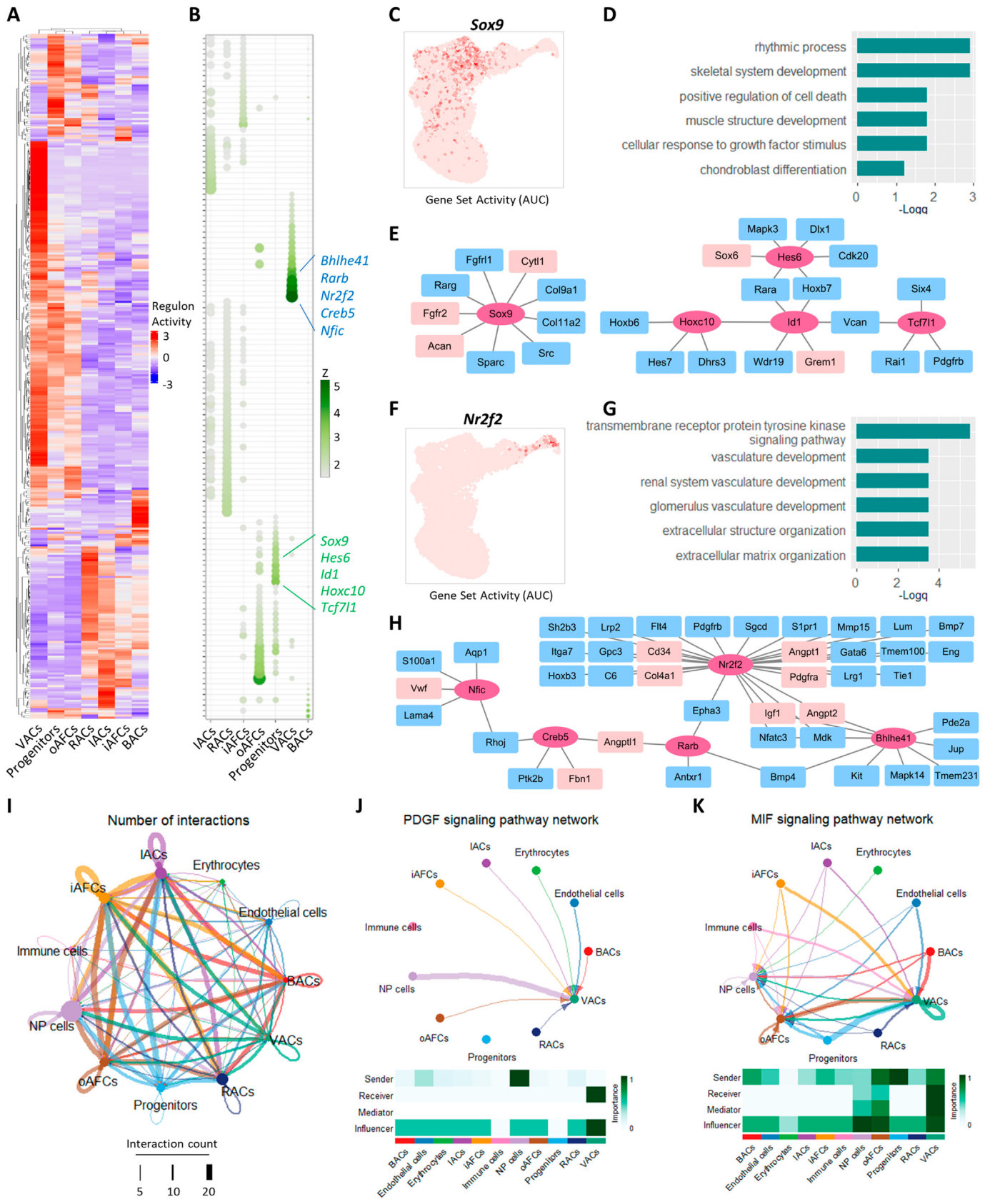

(caption on next page)

Figure 5. Gene regulation network and cell–cell interactions of the progenitor and vascularization-associated cell (VAC) subpopulations (A) Heatmap of the regulon activity in each AF cluster (B) Cell type-specific regulons of each cluster. The progenitor and VAC-specific regulons were marked by the key TF gene names with green and blue colors respectively (C) Featureplot showing the distribution of the representative regulon (indicated by the key TF *Sox9*) activity. Red color intensity indicates the activity level of the regulon in corresponding cells (D) Enriched GO terms of the top 5 regulon target genes in the progenitor subpopulation. The terms were ranked by -logq values (E) Regulation network of the key TFs and their target genes in the progenitor subpopulation. Red color indicates the key TFs; light red indicates stemness-related genes (F) Featureplot showing the distribution of the representative regulon (indicated by the key TF *Nr2f2*) activity. Red color intensity indicates the activity level of the regulon in corresponding cells (G) Enriched GO terms of the top 5 regulon target genes in the VAC subpopulation. The terms were ranked by -logq values (H) Regulation network of the key TFs and their target genes in the VAC subpopulation. Red color indicates the key TFs; light red indicates vascularization-related genes (I) Overview of the interactions of different IVD cell clusters. Dot size indicates the relative quantity of each cluster, and the thickness of the line indicates the relative quantity of significant ligand–receptor pairs between the linked clusters (J–K) Circle plots showing the inferred PDGF (J) and MIF (K) signaling networks. The heatmaps show the roles and the relative importance of each cluster in the networks.

Blood brings nutrition, oxygen, growth factors, and stem cells to the injured tissue; but it can also change the microenvironment, accompanied by inflammation and macrophage infiltration [75]. In bones, vascularization is a necessary process to promote tissue remodeling, which is critical in bone regeneration [76–78]. While for chondrocytes, the cells in another avascular tissue cartilage, short-term exposure to blood would lead to apoptosis [79], implying that vascularization may also contribute to IDD through regulating AF cells. The effect of blood vessels in degenerated IVDs should be investigated in future studies.

Although this study provides new information on mature AF resident cell subpopulations, limitations still exist. As cells usually do not proliferate, differentiate, and change states at a synchronous rate, it is possible that ancestral cells and their descendants, or activated cells and the quiescent siblings, present at the same timepoint. Since there was only one timepoint in this single-cell analysis, it is not certain if these cell populations identified are truly different, or just different states of the same cells. Additionally, these newly-discovered subpopulations were mainly characterized by single-cell RNA-seq analysis without further isolation and identification. It should be addressed in future studies.

In summary, this study looked into the rat IVD cell components and demonstrated the heterogeneity and multi-functions of the resident cells. The existence of the progenitors as well as the vascularization-associated cells in AF was demonstrated. These findings complement our knowledge about IVDs, especially the AF, and in return provide potential cell source and regulation targets for IDD treatment and tissue repair.

Funding

This work was supported by the Natural Science Foundation of China (81925027, 32130059), China Postdoctoral Science Foundation (2021M692356), Ningbo University Human Body Biomechanism Institute Open Foundation (CJ-HBIO202108), and the Priority Academic Program Development (PAPD) of Jiangsu Higher Education Institutions.

Author statement

Heng Sun: Conception and design of study, acquisition of data, analysis and/or interpretation of data, Drafting the manuscript. Huan Wang: acquisition of data. Weidong Zhang: acquisition of data. Haijiao Mao: Conception and design of study. Bin Li: Conception and design of study, revising the manuscript critically for important intellectual content.

Declaration of Competing interest

The authors declare that they have no known competing financial interests or personal relationships that could have appeared to influence the work reported in this paper.

Acknowledgements

The authors thank all the members of the orthopedic institute for their assistance of the data analysis experiment and manuscript preparation.All persons who have made substantial contributions to the work reported in the manuscript (e.g., technical help, writing and editing assistance, general support), but who do not meet the criteria for authorship, are named in the Acknowledgements and have given us their written permission to be named. If we have not included an Acknowledgements, then that indicates that we have not received substantial contributions from non-authors.

Appendix A. Supplementary data

Supplementary data to this article can be found online at https://doi.org/10.1016/j.jot.2022.11.004.

References

[1] Vlaeyen JWS, Maher CG, Wiech K, Van Zundert J, Meloto CB, Diatchenko L, et al. Low back pain. Nat Rev Dis Prim. 2018;4:1–18. https://doi.org/10.1038/s41572-018-0052-1.
[2] Hartvigsen J, Hancock MJ, Kongsted A, Louw Q, Ferreira ML, Genevay S, et al. What low back pain is and why we need to pay attention. Lancet 2018;391:2356–67. https://doi.org/10.1016/S0140-6736(18)30480-X.
[3] Du X-F, Cui H-T, Pan H-H, Long J, Cui H-W, Chen S-L, et al. Role of the miR-133a-5p/FBXO6 axis in the regulation of intervertebral disc degeneration. J Orthop Transl. 2021;29:123–33. https://doi.org/10.1016/j.jot.2021.05.004.
[4] Torre OM, Mroz V, Bartelstein MK, Huang AH, Iatridis JC. Annulus fibrosus cell phenotypes in homeostasis and injury: implications for regenerative strategies. Ann N Y Acad Sci. 2019;1442:61–78. https://doi.org/10.1111/nyas.13964.
[5] Wang H, Wang D, Luo B, Wang D, Jia H, Peng P, et al. Decoding the annulus fibrosus cell atlas by scRNA-seq to develop an inducible composite hydrogel: a novel strategy for disc reconstruction. Bioact Mater. 2022;14:350–63. https://doi.org/10.1016/j.bioactmat.2022.01.040.
[6] Guillamat-Prats R. The role of MSC in wound healing, scarring and regeneration. Cells 2021;10:1729. https://doi.org/10.3390/cells10071729.
[7] Hu B, He R, Ma K, Wang Z, Cui M, Hu H, et al. Intervertebral disc-derived stem/progenitor cells as a promising cell source for intervertebral disc regeneration. Stem Cell Int. 2018;2018:e7412304. https://doi.org/10.1155/2018/7412304.
[8] Chu G, Yuan Z, Zhu C, Zhou P, Wang H, Zhang W, et al. Substrate stiffness- and topography-dependent differentiation of annulus fibrosus-derived stem cells is regulated by Yes-associated protein. Acta Biomater. 2019;92:254–64. https://doi.org/10.1016/j.actbio.2019.05.013.
[9] Gan Y, He J, Zhu J, Xu Z, Wang Z, Yan J, et al. Spatially defined single-cell transcriptional profiling characterizes diverse chondrocyte subtypes and nucleus pulposus progenitors in human intervertebral discs. Bone Res 2021;9:1–15. https://doi.org/10.1038/s41413-021-00163-z.
[10] Wang J, Huang Y, Huang L, Shi K, Wang J, Zhu C, et al. Novel biomarkers of intervertebral disc cells and evidence of stem cells in the intervertebral disc. Osteoarthritis Cartilage 2021;29:389–401. https://doi.org/10.1016/j.joca.2020.12.005.
[11] Panebianco CJ, Dave A, Charytonowicz D, Sebra R, Iatridis JC. Single-cell RNA-sequencing atlas of bovine caudal intervertebral discs: discovery of heterogeneous cell populations with distinct roles in homeostasis. FASEB J. 2021;35:e21919. https://doi.org/10.1096/fj.202101149R.
[12] Calió M, Gantenbein B, Egli M, Poveda L, Ille F. The cellular composition of bovine coccygeal intervertebral discs: a comprehensive single-cell RNAseq analysis. Int J Mol Sci. 2021;22:4917. https://doi.org/10.3390/ijms22094917.
[13] Tu J, Li W, Yang S, Yang P, Yan Q, Wang S, et al. Single-cell transcriptome profiling reveals multicellular ecosystem of nucleus pulposus during degeneration progression. Adv Sci. 2022;9:2103631. https://doi.org/10.1002/advs.202103631.
[14] Worthley DL, Churchill M, Compton JT, Tailor Y, Rao M, Si Y, et al. Gremlin 1 identifies a skeletal stem cell with bone, cartilage, and reticular stromal potential. Cell 2015;160:269–84. https://doi.org/10.1016/j.cell.2014.11.042.
[15] Byvaltsev VA, Kolesnikov SI, Belykh EG, Stepanov IA, Kalinin AA, Bardonova LA, et al. Complex analysis of diffusion transport and microstructure of an intervertebral disk. Bull Exp Biol Med 2017;164:223–8. https://doi.org/10.1007/s10517-017-3963-z.
[16] Fournier DE, Kiser PK, Shoemaker JK, Battié MC, Séguin CA. Vascularization of the human intervertebral disc: a scoping review. JOR Spine 2020;3:e1123. https://doi.org/10.1002/jsp2.1123.

[17] Lama P, Maitre CLL, Harding IJ, Dolan P, Adams MA. Nerves and blood vessels in degenerated intervertebral discs are confined to physically disrupted tissue. J Anat 2018;233:86–97. https://doi.org/10.1111/joa.12817.
[18] Zhou Y, Zhou B, Pache L, Chang M, Khodabakhshi AH, Tanaseichuk O, et al. Metascape provides a biologist-oriented resource for the analysis of systems-level datasets. Nat Commun 2019;10:1523. https://doi.org/10.1038/s41467-019-09234-6.
[19] Grün D, Muraro MJ, Boisset J-C, Wiebrands K, Lyubimova A, Dharmadhikari G, et al. De novo prediction of stem cell identity using single-cell transcriptome data. Cell Stem Cell 2016;19:266–77. https://doi.org/10.1016/j.stem.2016.05.010.
[20] Owen RP, White MJ, Severson DT, Braden B, Bailey A, Goldin R, et al. Single cell RNA-seq reveals profound transcriptional similarity between Barrett's oesophagus and oesophageal submucosal glands. Nat Commun 2018;9:4261. https://doi.org/10.1038/s41467-018-06796-9.
[21] Trapnell C, Cacchiarelli D, Grimsby J, Pokharel P, Li S, Morse M, et al. The dynamics and regulators of cell fate decisions are revealed by pseudotemporal ordering of single cells. Nat Biotechnol 2014;32:381–6. https://doi.org/10.1038/nbt.2859.
[22] Qiu X, Hill A, Packer J, Lin D, Ma Y-A, Trapnell C. Single-cell mRNA quantification and differential analysis with Census. Nat Methods 2017;14:309–15. https://doi.org/10.1038/nmeth.4150.
[23] La Manno G, Soldatov R, Zeisel A, Braun E, Hochgerner H, Petukhov V, et al. RNA velocity of single cells. Nature 2018;560:494–8. https://doi.org/10.1038/s41586-018-0414-6.
[24] Aibar S, González-Blas CB, Moerman T, Huynh-Thu VA, Imrichova H, Hulselmans G, et al. SCENIC: single-cell regulatory network inference and clustering. Nat Methods 2017;14:1083–6. https://doi.org/10.1038/nmeth.4463.
[25] He J, Yan J, Wang J, Zhao L, Xin Q, Zeng Y, et al. Dissecting human embryonic skeletal stem cell ontogeny by single-cell transcriptomic and functional analyses. Cell Res 2021:1–16. https://doi.org/10.1038/s41422-021-00467-z.
[26] Jin S, Guerrero-Juarez CF, Zhang L, Chang I, Ramos R, Kuan C-H, et al. Inference and analysis of cell-cell communication using CellChat. Nat Commun 2021;12:1088. https://doi.org/10.1038/s41467-021-21246-9.
[27] Peng Y, Qing X, Shu H, Tian S, Yang W, Chen S, et al. Proper animal experimental designs for preclinical research of biomaterials for intervertebral disc regeneration. Biomater Transl 2021;2:91. https://doi.org/10.12336/biomatertransl.2021.02.003.
[28] Zhang W, Wang H, Yuan Z, Chu G, Sun H, Yu Z, et al. Moderate mechanical stimulation rescues degenerative annulus fibrosus by suppressing caveolin-1 mediated pro-inflammatory signaling pathway. Int J Biol Sci 2021;17:1395–412. https://doi.org/10.7150/ijbs.57774.
[29] Rutges J, Creemers LB, Dhert W, Milz S, Sakai D, Mochida J, et al. Variations in gene and protein expression in human nucleus pulposus in comparison with annulus fibrosus and cartilage cells: potential associations with aging and degeneration. Osteoarthritis Cartilage 2010;18:416–23. https://doi.org/10.1016/j.joca.2009.09.009.
[30] Lee CR, Sakai D, Nakai T, Toyama K, Mochida J, Alini M, et al. A phenotypic comparison of intervertebral disc and articular cartilage cells in the rat. Eur Spine J 2007;16:2174–85. https://doi.org/10.1007/s00586-007-0475-y.
[31] Rodrigues-Pinto R, Berry A, Piper-Hanley K, Hanley N, Richardson SM, Hoyland JA. Spatiotemporal analysis of putative notochordal cell markers reveals CD24 and keratins 8, 18, and 19 as notochord-specific markers during early human intervertebral disc development. J Orthop Res 2016;34:1327–40. https://doi.org/10.1002/jor.23205.
[32] Park-Windhol C, Ng YS, Yang J, Primo V, Saint-Geniez M, D'Amore PA. Endomucin inhibits VEGF-induced endothelial cell migration, growth, and morphogenesis by modulating VEGFR2 signaling. Sci Rep 2017;7:17138. https://doi.org/10.1038/s41598-017-16852-x.
[33] Schoonderwoerd MJA, Goumans M-JTH, Hawinkels LJAC. Endoglin: beyond the endothelium. Biomolecules 2020;10:289. https://doi.org/10.3390/biom10020289.
[34] Sauteur L, Krudewig A, Herwig L, Ehrenfeuchter N, Lenard A, Affolter M, et al. Cdh5/VE-cadherin promotes endothelial cell interface elongation via cortical Actin polymerization during angiogenic sprouting. Cell Rep 2014;9:504–13. https://doi.org/10.1016/j.celrep.2014.09.024.
[35] Crauwels P, Bank E, Walber B, Wenzel UA, Agerberth B, Chanyalew M, et al. Cathelicidin contributes to the restriction of leishmania in human host macrophages. Front Immunol 2019;10:2697. https://doi.org/10.3389/fimmu.2019.02697.
[36] Liao X, Shen Y, Zhang R, Sugi K, Vasudevan NT, Alaiti MA, et al. Distinct roles of resident and nonresident macrophages in nonischemic cardiomyopathy. Proc Natl Acad Sci USA 2018;115:E4661–9. https://doi.org/10.1073/pnas.1720065115.
[37] Hong J, Qu P, Wuest TR, Huang H, Huang C, Lin PC. Neutrophilic granule protein is a novel murine LPS antagonist. Immune Netw 2019;19:e34. https://doi.org/10.4110/in.2019.19.e34.
[38] Chen C-Z, Li M, Graaf D de, Monti S, Göttgens B, Sanchez M-J, et al. Identification of endoglin as a functional marker that defines long-term repopulating hematopoietic stem cells. Proc Natl Acad Sci USA 2002;99:15468–73. https://doi.org/10.1073/pnas.202614899.
[39] Morimoto R, Akeda K, Iida R, Nishimura A, Tsujii M, Obata S, et al. Tissue renin-angiotensin system in the intervertebral disc. Spine 2013;38:E129. https://doi.org/10.1097/BRS.0b013e31827b8c89.
[40] Lin L, Hu K. Tissue plasminogen activator and inflammation: from phenotype to signaling mechanisms. Am J Clin Exp Immunol 2014;3:30–6. https://www.ncbi.nlm.nih.gov/pmc/articles/PMC3960759/.
[41] Ferretti E, Tremblay E, Thibault M-P, Grynspan D, Burghardt KM, Bettolli M, et al. The nitric oxide synthase 2 pathway is targeted by both pro- and anti-inflammatory treatments in the immature human intestine. Nitric Oxide 2017;66:53–61. https://doi.org/10.1016/j.niox.2017.03.003.
[42] Ross D, Siegel D. Functions of NQO1 in cellular protection and CoQ10 metabolism and its potential role as a redox sensitive molecular switch. Front Physiol 2017;8:595. https://doi.org/10.3389/fphys.2017.00595.
[43] Lee D, Xu IM-J, Chiu DK-C, Leibold J, Tse AP-W, Bao MH-R, et al. Induction of oxidative stress through inhibition of thioredoxin reductase 1 is an effective therapeutic approach for hepatocellular carcinoma. Hepatology 2019;69:1768–86. https://doi.org/10.1002/hep.30467.
[44] Ursini F, Maiorino M, Forman HJ. Redox homeostasis: the golden mean of healthy living. Redox Biol 2016;8:205–15. https://doi.org/10.1016/j.redox.2016.01.010.
[45] Medzhitov R. Origin and physiological roles of inflammation. Nature 2008;454:428–35. https://doi.org/10.1038/nature07201.
[46] Asp J, Thornemo M, Inerot S, Lindahl A. The helix-loop-helix transcription factors Id1 and Id3 have a functional role in control of cell division in human normal and neoplastic chondrocytes. FEBS Lett 1998;438:85–90. https://doi.org/10.1016/S0014-5793(98)01268-X.
[47] Thornemo M, Jansson ES, Lindahl A. Expression of the ID1 and ID3 genes during chondrocyte differentiation. Ann N Y Acad Sci 1996;785:337–9. https://doi.org/10.1111/j.1749-6632.1996.tb56302.x.
[48] Roschger C, Cabrele C. The Id-protein family in developmental and cancer-associated pathways. Cell Commun Signal 2017;15:7. https://doi.org/10.1186/s12964-016-0161-y.
[49] Holmfeldt P, Ganuza M, Marathe H, He B, Hall T, Kang G, et al. Functional screen identifies regulators of murine hematopoietic stem cell repopulation. J Exp Med 2016;213:433–49. https://doi.org/10.1084/jem.20150806.
[50] Jeon J, Oh H, Lee G, Ryu J-H, Rhee J, Kim J-H, et al. Cytokine-like 1 knock-out mice (Cytl1−/−) show normal cartilage and bone development but exhibit augmented osteoarthritic cartilage destruction. J Biol Chem 2011;286:27206–13. https://doi.org/10.1074/jbc.M111.218065.
[51] Chen J, Zhang E, Zhang W, Liu Z, Lu P, Zhu T, et al. Fos promotes early stage teno-lineage differentiation of tendon stem/progenitor cells in tendon. STEM CELLS Transl Med 2017;6. https://doi.org/10.1002/sctm.15-0146. 2009–19.
[52] Lin S, Zhang Q, Shao X, Zhang T, Xue C, Shi S, et al. IGF-1 promotes angiogenesis in endothelial cells/adipose-derived stem cells co-culture system with activation of PI3K/Akt signal pathway. Cell Prolif 2017;50:e12390. https://doi.org/10.1111/cpr.12390.
[53] Carbone C, Piro G, Merz V, Simionato F, Santoro R, Zecchetto C, et al. Angiopoietin-like proteins in angiogenesis, inflammation and cancer. Int J Mol Sci 2018;19:431. https://doi.org/10.3390/ijms19020431.
[54] Wei S-T, Huang Y-C, Hsieh M-L, Lin Y-J, Shyu W-C, Chen H-C, et al. Atypical chemokine receptor ACKR3/CXCR7 controls postnatal vasculogenesis and arterial specification by mesenchymal stem cells via Notch signaling. Cell Death Dis 2020;11:1–17. https://doi.org/10.1038/s41419-020-2512-2.
[55] Horikawa S, Ishii Y, Hamashima T, Yamamoto S, Mori H, Fujimori T, et al. PDGFRα plays a crucial role in connective tissue remodeling. Sci Rep 2015;5:17948. https://doi.org/10.1038/srep17948.
[56] Xu J, Shi G-P. Vascular wall extracellular matrix proteins and vascular diseases. Biochim Biophys Acta 2014;1842:2106–19. https://doi.org/10.1016/j.bbadis.2014.07.008.
[57] Żak M, Pezowicz C. Effect of overload on changes in mechanical and structural properties of the annulus fibrosus of the intervertebral disc. Biomech Model Mechanobiol 2021;20:2259–67. https://doi.org/10.1007/s10237-021-01505-w.
[58] Moreira S, Polena E, Gordon V, Abdulla S, Mahendram S, Cao J, et al. A single TCF transcription factor, regardless of its activation capacity, is sufficient for effective trilineage differentiation of ESCs. Cell Rep 2017;20:2424–38. https://doi.org/10.1016/j.celrep.2017.08.043.
[59] Formeister EJ, Sionas AL, Lorance DK, Barkley CL, Lee GH, Magness ST. Distinct SOX9 levels differentially mark stem/progenitor populations and enteroendocrine cells of the small intestine epithelium. Am J Physiol Gastrointest Liver Physiol 2009;296:G1108–18. https://doi.org/10.1152/ajpgi.00004.2009.
[60] Aguilar-Medina M, Avendaño-Félix M, Lizárraga-Verdugo E, Bermúdez M, Romero-Quintana JG, Ramos-Payan R, et al. SOX9 stem-cell factor: clinical and functional relevance in cancer. JAMA Oncol 2019;2019:6754040. https://doi.org/10.1155/2019/6754040.
[61] Sissaoui S, Yu J, Yan A, Li R, Yukselen O, Kucukural A, et al. Genomic characterization of endothelial enhancers reveals a multifunctional role for NR2F2 in regulation of arteriovenous gene expression. Circ Res 2020;126:875–88. https://doi.org/10.1161/CIRCRESAHA.119.316075.
[62] Wang S, Qiu J, Liu L, Su C, Qi L, Huang C, et al. CREB5 promotes invasiveness and metastasis in colorectal cancer by directly activating MET. J Exp Clin Cancer Res 2020;39:168. https://doi.org/10.1186/s13046-020-01673-0.
[63] Abu El-Asrar AM, Ahmad A, Siddiquei MM, De Zutter A, Allegaert E, Gikandi PW, et al. The proinflammatory and proangiogenic macrophage migration inhibitory factor is a potential regulator in proliferative diabetic retinopathy. Front Immunol 2019;10. https://doi.org/10.3389/fimmu.2019.02752.
[64] Nagao M, Feinstein TN, Ezura Y, Hayata T, Notomi T, Saita Y, et al. Sympathetic control of bone mass regulated by osteopontin. Proc Natl Acad Sci USA 2011;108:17767–72. https://doi.org/10.1073/pnas.1109402108.
[65] Wei T, Bi G, Bian Y, Ruan S, Yuan G, Xie H, et al. The significance of secreted phosphoprotein 1 in multiple human cancers. Front Mol Biosci 2020;7:565383. https://doi.org/10.3389/fmolb.2020.565383.
[66] Erikson DW, Burghardt RC, Bayless KJ, Johnson GA. Secreted phosphoprotein 1 (SPP1, Osteopontin) binds to Integrin alphavbeta6 on porcine trophectoderm cells and Integrin alphavbeta3 on uterine luminal epithelial cells, and promotes

trophectoderm cell adhesion and migration. Biol Reprod 2009;81:814–25. https://doi.org/10.1095/biolreprod.109.078600.
[67] Romero-Lanman EE, Pavlovic S, Amlani B, Chin Y, Benezra R. Id1 maintains embryonic stem cell self-renewal by up-regulation of Nanog and repression of Brachyury expression. Stem Cell Dev 2012;21:384–93. https://doi.org/10.1089/scd.2011.0428.
[68] Chu G, Zhang W, Zhou P, Yuan Z, Zhu C, Wang H, et al. Substrate topography regulates differentiation of annulus fibrosus-derived stem cells via CAV1-YAP-mediated mechanotransduction. ACS Biomater Sci Eng 2021;7:862–71. https://doi.org/10.1021/acsbiomaterials.9b01823.
[69] Rudert M, Tillmann B. Detection of lymph and blood vessels in the human intervertebral disc by histochemical and immunohistochemical methods. Ann Anat 1993;175:237–42. https://doi.org/10.1016/S0940-9602(11)80009-9.
[70] Rätsep T, Minajeva A, Asser T. Relationship between neovascularization and degenerative changes in herniated lumbar intervertebral discs. Eur Spine J 2013;22:2474–80. https://doi.org/10.1007/s00586-013-2842-1.
[71] Karamouzian S, Eskandary H, Saeed A, Reihani-Kermani H, Aboosaeedi HR, Malekpoor-Afshar R, et al. Effect of atorvastatin on angiogenesis in degenerated intervertebral disc in rat. Spine 2011;36:1824–8. https://doi.org/10.1097/BRS.0b013e3181d4e15a.
[72] Feng G, Yang X, Shang H, Marks IW, Shen FH, Katz A, et al. Multipotential differentiation of human anulus fibrosus cells: an in vitro study. J Bone Joint Surg 2010;92:675–85. https://doi.org/10.2106/JBJS.H.01672.
[73] Maitre CLL, Richardson SM, Baird P, Freemont AJ, Hoyland JA. Expression of receptors for putative anabolic growth factors in human intervertebral disc: implications for repair and regeneration of the disc. J Pathol 2005;207:445–52. https://doi.org/10.1002/path.1862.
[74] Gerthoffer WT. Mechanisms of vascular smooth muscle cell migration. Circ Res 2007;100:607–21. https://doi.org/10.1161/01.RES.0000258492.96097.47.
[75] Koike Y, Uzuki M, Kokubun S, Sawai T. Angiogenesis and inflammatory cell infiltration in lumbar disc herniation. Spine 2003;28:1928–33. https://doi.org/10.1097/01.BRS.0000083324.65405.AE.
[76] Filipowska J, Tomaszewski KA, Ł Niedźwiedzki, Walocha JA, Niedźwiedzki T. The role of vasculature in bone development, regeneration and proper systemic functioning. Angiogenesis 2017;20:291–302. https://doi.org/10.1007/s10456-017-9541-1.
[77] Li Y, Pan Q, Xu J, He X, Li HA, Oldridge DA, et al. Overview of methods for enhancing bone regeneration in distraction osteogenesis: potential roles of biometals. J Orthop Transl 2021;27:110–8. https://doi.org/10.1016/j.jot.2020.11.008.
[78] Cheng W-X, Liu Y-Z, Meng X-B, Zheng Z-T, Li L-L, Ke L-Q, et al. PLGA/β-TCP composite scaffold incorporating cucurbitacin B promotes bone regeneration by inducing angiogenesis. J Orthop Transl 2021;31:41–51. https://doi.org/10.1016/j.jot.2021.10.002.
[79] Hooiveld M, Roosendaal G, Wenting M, van den Berg M, Bijlsma J, Lafeber F. Short-term exposure of cartilage to blood results in chondrocyte apoptosis. Am J Pathol 2003;162:943–51. https://doi.org/10.1016/S0002-9440(10)63889-8.